The Use of Frequency Dependent Trigonometric Shape Functions in Vibration Analysis of Beam Structures - Bridging Gap Between FEM and Exact DSM Formulations

By:

S. M. Hashemi, Assistant Peofessor,

Department of Aerospace Engineering,
Ryerson University, 350 Victoria Street, Toronto (ON) Canada

ABSTRACT

The free vibration of flexible beam structures is revisited. Based on the Euler-Bernoulli and St-Venant beam theories, the differential equations governing coupled extensional, torsional, and flexural vibrations of axially loaded beams are first reviewed. The `exact' analytical formulation, based on the closed form solution of these equations is then discussed. This formulation leads to the well-known Dynamic Stiffness Matrix (DSM) method. Based on the Finite Element Methodology, and neglecting geometric couplings, the Dynamic (frequency dependent) Trigonometric Shape Functions (DTSFs) for the beam's uncoupled displacements are thereafter derived. Consequently, exploiting the Principle of Virtual Work (PVW) and interpolating the variables based on the DTSF, the exact Dynamic Finite Element (DFE) formulations for uniform beams' axial and pure bending vibrations are developed. The method of incorporating different coupling effects, as well as variable geometrical and mechanical parameters in DFE formulation is also discussed. The applicability of the DFE method is then demonstrated by three illustrative examples where a Wittrick-Williams root counting technique is used to find the systems' natural frequencies. The DFE, as an intermediate method, can bridge the gap between FEM and DSM formulations and can be advantageously used when the multiple natural frequencies and/or higher modes of beam structures are to be evaluated.

1. Introduction

Many mechanical systems as well as numerous terrestrial and aerospace structures can be modeled as axially loaded slender coupled beams or beam assemblies. Different authors have studied the dynamic modeling and the equations of motion for vibrations of various beam configurations and a variety of approaches for the frequency calculation of these structures have been proposed. Some good literature surveys have been published in different occasions

(see, for example, Reference [1]). One can also find in Reference [2] a review of approximate methods such as Mykelstad method, the Galerkin approach, the Rayleigh-Ritz method, the finite element formulation, etc., with a special regard to blades analysis. The classical Finite Element Method (FEM), where beam element matrices are evaluated from assumed fixed (namely polynomial) shape functions, has been widely used by investigators [1,3]. This practice results in approximate equations in the form of mass and static stiffness matrices. A deviation from the conventional FEM formulation would pay dividends if improved accuracy of results can be obtained by using shape functions other than polynomials. This is the case when the homogeneous solution of the pertinent differential equation is available for the development of each element matrices. For static analysis, the use of the homogeneous solution of the differential equation yields the exact stiffness matrix and load vector for a beam element [4]. The use of other alternative shape functions in dynamic FEM formulations have also been explored.

The Dynamic Stiffness Matrix (DSM) method offers a better alternative particularly when higher frequencies and better accuracies of results are required. It relies on a single frequency dependent matrix which has both mass and stiffness properties. The use of a DSM in vibration analysis is well established [5-7]. Obviously the method gives more accurate results because it exploits the exact member theory. The matrix is obtained by directly solving the governing differential equation. That is why the results obtained by DSM are often justifiably called “exact” [7]. Other methods have been also explored and reported in scientific literatures that are more or less similar to those explained previously. Some of them were developed to treat a particular configuration and group of mechanical systems.

A thorough investigation of the existing conventional FEM and alternative DSM methods in beam vibrations has led to the development of Dynamic (frequency dependent) Finite Element (DFE) approach. DFE can bridge the gap between the standard FEM and the exact DSM methods by advantageously exploiting the generality of FEM and the very precise frequency calculations provided by DSM approach. From this point of view, the method retains the physical aspect of analytical or semi-analytical approaches and the power of a numerical method. It has been shown that DFE is an efficient tool for handling periodical structures or systems composed of several identical substructures. In this case, all substructures have the same dynamic stiffness components and frequency characteristics so that increasing the number of substructures does not significantly increase the computation time. Here, we first investigate the coupled extensional, torsional and flap Bending vibrations of a beam in presence of a constant axial load. The exact DSM, FEM and DFE formulations of the problem,

for simple cases, are then presented. This will help to achieve a better understanding of DFE approach and to prepare the terrain for the development of DFE formulation for more complex cases where the exact solutions are not available. For this purpose, the differential equations governing the uncoupled displacements of an axially loaded uniform beam element are solved in an exact sense. Then, the resulting solutions are used as the basis functions to derive the frequency dependent Dynamic Trigonometric Shape Functions (DTSFs) that are later used to derive the corresponding stiffness matrices. Exploiting the weighted residual method and using the variables' nodal approximation based on the DTSFs, the effects of variable axial force, geometrical parameters and mechanical properties, are incorporated into the DFE formulation. Finally, application of the theory is demonstrated by three illustrative examples of beam configurations wherein (a) substantial amount of coupling between bending and torsion, (b) tapered geometry, and (c) distributed centrifugal axial force are highlighted. The natural frequencies are evaluated for each configuration and are compared with previously published results to confirm the accuracy of the method, and some conclusions are drawn.

2. Theory

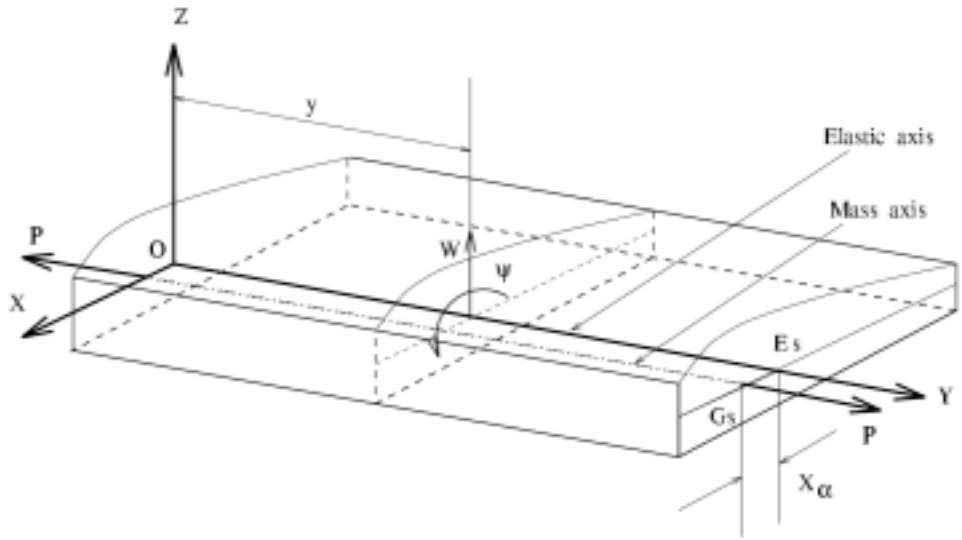

Figure 1. Coordinate system and notations for coupled bending-torsion vibration of an axially loaded uniform beam element: E_s **shear centre;** G_s **mass centre.**

The governing differential equations of motion for an axially loaded uniform beam with an open or closed thin-walled cross-section of the type shown in Figure1 is presented in references [8,9]. The Shear deformation, warping and rotary inertia effects are neglected. In the right handed coordinate system shown in Figure 1, the elastic axis which is assumed to be coincident with the x-axis is permitted axial deformation $u(x,t)$, lateral translation $w(x,t)$ in the z-direction and rotation $\psi(x,t)$ about x-axis (torsion). The mass and elastic axes are separated by a distance x_α. x and t denote distance from the origin and time, respectively. A constant axial load P is assumed to act through the centroid (mass centre) of the cross section. P is considered to be positive when tensional, as shown in the figure (P can be positive or negative. Hence compression is also included). Assuming sinusoidal variation of w and ψ, with circular frequency ω,

$$u(x,t) = u(x)\sin(\omega t);\quad w(x,t) = w(x)\sin(\omega t);\quad \psi(x,t) = \psi(x)\sin(\omega t) \tag{1}$$

the differential equations governing the beam vibrations (see Figure 1) are [8]:

$$(-H_m u')' - m\omega^2 u = 0 \tag{2}$$

$$(H_f w'')'' - (Pw')' - m\omega^2 w + [(Px_\alpha \psi')' + mx_\alpha \omega^2 \psi] = 0 \tag{3}$$

$$[-(H_t + P(I_\alpha/m))\psi']' - I_\alpha \omega^2 \psi + [(Px_\alpha w')' + mx_\alpha \omega^2 w] = 0 \tag{4}$$

where $u(x)$, $w(x)$ and $\psi(x)$ are the amplitudes of the sinusoidally varying axial and vertical displacements and torsional rotation respectively. $H_m = EA$, $H_f = EI$ and $H_t = GJ$ are the membrane, bending and torsional rigidity of the beam, respectively; $m = \rho A$ is the mass per unit length, I_α is the polar mass moment of inertia per unit length about the x-axis (i.e., shear axis) and primes denote time and differentiation with respect to position x. The appropriate boundary conditions are imposed at $x = 0, L$. For example: Clamped at $x = 0$; $u = w = w' = \psi = 0$, Free at $x = L$; $u' = w'' = w''' = \psi' = 0$, etc.

The resultant axial force, *N(x)*, shear force, *T(x)*, bending moment, $M_F(x)$, and torsioal moment, $M_T(x)$, are:

$$N(x) = H_m u';\quad T(x) = (-H_f w'')' + P(w' - x_\alpha \psi') \tag{5}$$

$$M_F(x) = -H_f w'';\quad M_T(x) = (H_t + P(I_\alpha / m))\psi' - (Px_\alpha)w' \tag{6}$$

3 Dynamic Modeling and Formulation

From the theory presented in the previous section it can be realized that the axial force does not have any effects on the beam's axial vibration. Moreover, since there is no coupling between the axial and the lateral deformations, the membrane deformation and bending-torsion vibrations could be treated separately.

3.1 Frequency Dependent Dynamic Stiffness Matrix (DSM) Formulation

In the following, the derivation of the exact DSM for the axial vibration of a pre-stressed beam element, governed by eqn (2), is briefly discussed. Similarly, one could exploit the DSM approach to analyze the beam uncoupled bending, torsion, and coupled bending-torsion vibrations governed by eqns (3) and (4) (see Appendix A for a brief formulation) [5,7].

3.1.1 Exact DSM for the Axial Vibration of Beams

Assuming the beam as the assembly of elements with homogeneous material and uniform geometry, eqn (2) can be written as

$$\left(-H_m D^2 - m\omega^2 l^2\right)u = 0; \text{ where } D = d/d\xi \text{ and } \xi = x/l. \tag{7}$$

The solution of the differential eqn (5) is obtained as

$$u(\xi,\eta(\omega)) =< P(\xi,\eta(\omega)) >\{A\} \text{ and } < P(\xi,\eta(\omega)) >=< \cos(\eta(\omega).\xi) \ \sin(\eta(\omega).\xi) > \tag{8}$$

where $\{A\} =< A_1 \ A_2 >^T$ are arbitrary coefficients, $\eta^2(\omega) = \frac{\rho\omega^2}{E}$, and $l = x_{j+1} - x_j$. Then, the resulting normal force is

$$N(\xi,\eta(\omega)) = (H_m/L)\frac{du(\xi,\eta(\omega))}{d\xi} = (H_m/L) < P(\xi,\eta(\omega))_{,\xi} >\{A\} \tag{9}$$

The end conditions for displacements and forces of the beam element are respectively given as follows:

$$\begin{aligned} &\text{at end 1 (i.e., at } \xi = 0\text{); } u = u_1 \quad \text{and} \quad \text{at end 2 (i.e., at } \xi = 1\text{); } u = u_2; \\ &\text{at end 1 (i.e., at } \xi = 0\text{); } N = -N_1 \quad \text{and} \quad \text{at end 2 (i.e., at } \xi = 1\text{); } N = N_2. \end{aligned}$$

Substituting these boundary conditions in eqns (6) and (7)

$$\begin{Bmatrix} u_1 \\ u_2 \end{Bmatrix} = \begin{bmatrix} < P(\xi,\eta(\omega)) >_{(\xi=0)} \\ < P(\xi,\eta(\omega)) >_{(\xi=1)} \end{bmatrix} \begin{Bmatrix} A_1 \\ A_2 \end{Bmatrix} \qquad (\text{i.e.}, U_n = BA) \tag{8}$$

Then, from eqns (6–8) we can write

$$\begin{Bmatrix} N_1 \\ N_2 \end{Bmatrix} = \begin{bmatrix} -(H_m/L) < P(\xi,\eta(\omega))_{,\xi} >_{(\xi=0)} \\ (H_m/L) < P(\xi,\eta(\omega))_{,\xi} >_{(\xi=1)} \end{bmatrix} \begin{Bmatrix} A_1 \\ A_2 \end{Bmatrix} \qquad (\text{i.e.}, F = DA) \qquad (9)$$

and eqns (8) and (9) lead to

$$\begin{Bmatrix} N_1 \\ N_2 \end{Bmatrix} = \begin{bmatrix} k_{11} & k_{12} \\ sym. & k_{22} \end{bmatrix} \begin{Bmatrix} u_1 \\ u_2 \end{Bmatrix} \qquad (\text{i.e.}, F = KU_n) \qquad (10)$$

The 'exact' frequency dependent stiffness matrix for the beam's axial vibration, is

$$[k(\eta(\omega))] = \frac{H_m \eta}{L \sin \eta l} \begin{bmatrix} \cos(L\eta(\omega)) & -1 \\ -1 & \cos(L\eta(\omega)) \end{bmatrix} \qquad (\text{i.e.}, K = DB^{-1}) \qquad (11)$$

This matrix, together with the boundary conditions and an appropriate solution method leads to infinite number of exact natural frequencies and modes of beam axial vibrations.

3.2 Weak Integral Formulation

The Galerkin weak form associated to eqns (2-4) can be written as:

$$W = W_{INT} - W_{EXT} = \left(W_f + W_t + W_m\right) - W_{EXT} = 0 \qquad (12)$$

where, for free vibration analysis, $W_{EXT} = 0$. If the domain is discretized by a number of 2-node elements, then

$$W_{INT} = \sum_{k=1}^{NET} W^e \quad \text{where} \quad W^e = W^e{}_m + W^e{}_t + W^e{}_f \; ; \qquad (13)$$

and

$$W^e{}_m = \int_{x_j}^{x_{j+1}} \left\{ \delta u'(H_m) u' - \delta u (m\omega^2) u \right\} dx \qquad (14)$$

$$W^e{}_f = \int_{x_j}^{x_{j+1}} \left\{ \delta w''(H_f) w'' + \delta w'(P) w' - \delta w (m\omega^2) w - \delta w'(P x_\alpha) \psi' + \delta w \left(m x_\alpha \omega^2 \right) \psi \right\} dx \qquad (15)$$

$$W^e{}_t = \int_{x_j}^{x_{j+1}} \left\{ \delta \psi'(H_t + P(I_\alpha/m)) \psi' - \delta \psi (I_\alpha \omega^2) \psi - \delta \psi'(P x_\alpha) w' + \delta \psi \left(m x_\alpha \omega^2 \right) w \right\} dx \qquad (16)$$

Here, u, w and ψ are solution functions and δu, δw and $\delta \psi$ are test functions. Both quantities are defined in same approximation space. Each element is defined by nodes $j, j+1$ with corresponding coordinates. For Clamped-Free boundary conditions: $\delta u = \delta w = \delta w' = \delta \psi = 0$ at $x = 0$, and force terms are zero at $x = L$. The admissibility condition for finite element approximation is controlled by eqns (13-16).

Figure 2. Domain discretized by a number of 2-node elements.

3.2.1 Axial Vibration of Beams: 'Exact' Dynamic Finite Element (DFE)

In this section, the application of the Dynamic Finite Element (DFE) procedure to beam axial vibration is presented. The formulation presented here results in the same exact frequency dependent formulation and stiffness matrix as that obtained from the exact beam Dynamic Stiffness Matrix (DSM) formulation (see section 3.1.1). This procedure can easily be extended to develop the DFE formulation and the relevant matrices for the different cases such as pure torsion and bending of axially loaded uniform and tapered beams [5,10,11]. Consider again the beam axial vibration as governed by strong form of governing differential eqns (2 or 7) and appropriate boundary conditions at $x = 0$ and L. As previously shown, the weak integral form of the governing equation can be written as (see eqn 14):

$$W^e{}_m = \int_{x_j}^{x_{j+1}} \left\{ \delta u'(H_m) u' - \delta u (m\omega^2) u \right\} dx \tag{17}$$

This is the discretized (element) Galerkin weak form formulation of the governing eqn(2), which also satisfies the principle of virtual work as

$$W_m = W_{m\ INT} - W_{m\ EXT} = 0; \ \text{ where } \ W_{m\ INT} = \sum_{e=1}^{NE} W_m^e \tag{18}$$

Here, u and δu are the variable and the test functions, respectively. Both quantities are expressed by the same approximation space and $W_{m\ EXT} = 0$ for free vibrations. After another integration by parts, and assuming a uniform homogeneous element (i.e., constant E, ρ and A), expression (17) can be then written in the following form:

$$W^e = -\int_{x_j}^{x_{j+1}} \left\{ \delta u_{,xx} H_m + \delta u m \omega^2 \right\} u dx + [\delta u_{,x} H_m u]_{x_j}^{x_{j+1}} \tag{19}$$

Assuming

$$\delta u(x) = < P > \{\delta A\}, \ u(x) = < P > \{A\} \quad \text{and} \quad < P > = < \cos \eta x \ \ \tfrac{\sin \eta x}{\alpha} >, \tag{20}$$

the integral expression in eqn (19) cancels out. Then, the nodal approximation for the variables is written as:

$$\delta u(x) = < N(x,\eta) > \{\delta U_n\}; \quad < N(x,\eta) > = < P > [P_n]^{-1}; \tag{21}$$

where the nodal matrix, $[P_n]$, and interpolation functions, $< N(x,\eta) >$, are

$$[P_n] = \begin{bmatrix} 1 & 0 \\ \cos \eta l & (\sin \eta l)/\eta \end{bmatrix}; \quad < N(x,\eta) > \ = \ < \frac{\sin \eta (l-x)}{\sin \eta l} \quad \frac{\sin \eta x}{\sin \eta l} >. \tag{22}$$

Combining eqns (19) to (22), the (dynamic) stiffness matrix is obtained as:

$$W_m{}^e = H_m [\delta u_{,x} u]_{x_j}^{x_{j+1}} = H_m [(-\delta u_{,x})_1 u_1 + (\delta u_{,x})_2 u_2] = < \delta u_n > [k(\eta)] \{u_n\} \tag{23}$$

where

$$[k(\eta)] = H_m \begin{bmatrix} (-N_{1,x})_{x=0} & (N_{1,x})_{x=l} \\ (-N_{2,x})_{x=0} & (N_{2,x})_{x=l} \end{bmatrix} = \frac{H_m \eta}{l \sin \eta l} \begin{bmatrix} \cos \eta l & -1 \\ -1 & \cos \eta l \end{bmatrix}$$

Here $\eta^2 = \frac{\rho \omega^2}{E}$ and $l = x_{j+1} - x_j$. One can also use $\xi = x/l$ to write the above expressions in terms of element local coordinates. It can be verified that if expression (23) is developed as a series of function of η^2 [11], then

$$[k(\eta)] = [k(\eta \to 0)] - \eta^2 [m] - \eta^4 [m_1] \ldots \tag{24}$$

The first two terms correspond to the dynamic stiffness matrix obtained by the classical Finite Element Method (FEM) [10,11].

$$[k(\omega^2)] = H_m([k] - \omega^2 [m]) \tag{25}$$

where $[k(\eta \to 0)]$ and $[m]$ are the static stiffness and mass matrices. Similar developments in series, for some vibration problems, are also presented by [12].

3.2.2 Coupled Bending-Torsion Vibration of Beams: Dynamic Finite Element (DFE)

Consider the coupled bending-torsion vibrations of a pre-stressed beam governed by equations (3,4). The integral form of the element equations then is

$$W^e{}_f = \int_{x_j}^{x_{j+1}} \left\{ \delta w''(H_f) w'' + \delta w'(P) w' - \delta w (m\omega^2) w - \delta w' (P x_\alpha) \psi' + \delta w \left(m x_\alpha \omega^2 \right) \psi \right\} dx \tag{26}$$

$$W^e{}_t = \int_{x_j}^{x_{j+1}} \left\{ \delta \psi' (H_t + P(I_\alpha / m)) \psi' - \delta \psi (I_\alpha \omega^2) \psi - \delta \psi' (P x_\alpha) w' + \delta \psi \left(m x_\alpha \omega^2 \right) w \right\} dx \tag{27}$$

The components of (26) and (27) may also be written in an *equivalent form* obtained after integration by parts on each element:

$$\begin{aligned} W^e{}_f = & \int_0^1 w \underbrace{\left\{ \left(\frac{H_f}{l_k^3}\right) \delta w''' - \left(\frac{P}{l_k}\right) \delta w'' - (l_k m \omega^2) \delta w \right\}}_{(I)} d\xi + \\ & \left[\frac{H_f}{l_k^3} (\delta w'' w' - \delta w''' w) + \left(\frac{P}{l_k}\right) \delta w' w \right]_0^1 + \int_0^1 \left\{ \left(\frac{-P x_\alpha}{l_k}\right) \delta w' \psi' + (m l_k x_\alpha \omega^2) \delta w \psi' \right\} d\xi \end{aligned} \tag{28}$$

$$\begin{aligned} W^e{}_t = & \int_0^1 -\psi \underbrace{\left\{ \left(\frac{H_t + P(I_\alpha/m)}{l_k}\right) \delta \psi'' + (l_k I_\alpha \omega^2) \delta \psi \right\}}_{(II)} d\xi \\ & \left[\left(\frac{H_t + P I_\alpha / m}{l_k}\right) \delta \psi' \psi \right]_0^1 + \int_0^1 \left\{ \frac{-P x_\alpha}{l_k} \delta \psi' w' + (m l_k x_\alpha \omega^2) \delta \psi w \right\} d\xi \end{aligned} \tag{29}$$

where $\xi = x/l_k$. The admissibility condition for finite element approximation is controlled by

eqns (26,27); The lateral displacement variable and test functions require C^1 continuity condition assuring continuity of w and $w_{,x}$, whereas a C^0-type approximation space will guarantee the continuity of torsional displacement and test functions at each node. One can then use the solutions of the integral terms (I) and (II) in expressions (28,29) as basis functions of approximation space to develop the appropriate shape (interpolation) functions. The procedure is briefly explained here.

The non-nodal approximation of the solution function W, Ψ , and the test function $\delta w, \delta\Psi$, can be written as:

$$\delta W =< P(\xi) >_f \{\delta a\}; \;\; W =< P(\xi) >_f \{a\}$$
$$\delta\Psi =< P(\xi) >_t \{\delta b\}; \;\; \Psi =< P(\xi) >_t \{b\}$$

where the basis functions (i.e., expansion terms) of the approximation are

$$< P(\xi) >_f =< Cos(\alpha\xi) \;\; \frac{Sin(\alpha\xi)}{\alpha} \;\; \frac{Cosh(\beta\xi) - Cos(\alpha\xi)}{\alpha^2 + \beta^2} \;\; \frac{Sinh(\beta\xi) - Sin(\alpha\xi)}{\alpha^3 + \beta^3} >,$$
$$< P(\xi) >_t =< \cos(\tau\xi) \;\; \sin(\tau\xi)/\tau >. \qquad (30)$$

which are spoliations of the first integral terms (I) and (II) in eqns (25, 26). In addition, they are chosen in such manner that when α, β and $\tau \to 0$, they lead to classical basis functions of the standard beam element, based on the cubic "Hermite" type interpolation polynomials (for the bending), and the linear ones (for the torsion), respectively. Here;

$$\alpha, \beta = \frac{1}{\sqrt{2A}} \sqrt{|-B \pm \sqrt{|B^2 - 4AC|}|}, \;\; \tau = \sqrt{I_\alpha \omega^2 / H_t}, \qquad (31)$$

where $A = H_f / l_k^3$, $B = -(P/l_k)$, and $C = -(m l_k \omega^2)$. Note that the generalized parameters of the approximation have, in general, no direct physical meaning. Thus, $< \delta a >$, $< a >$ and $< \delta b >$, $< b >$ are more conveniently replaced by nodal variables; $< \delta W_1 \;\; \delta W_{,1} \delta W_2 \;\; \delta W_{,2} >$, $< W_1 \;\; W_{,1} \;\; W_2 \;\; W_{,2} >$ and $< \delta\Psi_1 \delta\Psi_2 >$, $< \Psi_1 \Psi_2 >$, respectively. Consequently, one can write (regarding Equations (27-29)):

$$\{W_n\} = [P_n]_f \{a\}; \;\; \{\delta W_n\} = [P_n]_f \{\delta a\}; \;\; \{\Psi_n\} = [P_n]_t \{b\}; \;\; \{\delta\Psi_n\} = [P_n]_t \{\delta b\} \qquad (32)$$

where

$$[P_n]_f = \begin{bmatrix} 1 & 0 & 0 & 0 \\ 0 & 1 & 0 & \dfrac{(\beta-\alpha)}{(\alpha^3+\beta^3)} \\ \cos(\alpha) & \dfrac{\sin(\alpha)}{\alpha} & \dfrac{[\cosh(\beta)-\cos(\alpha)]}{(\alpha^2+\beta^2)} & \dfrac{[\sinh(\beta)-\sin(\alpha)]}{(\alpha^3+\beta^3)} \\ -\alpha\sin(\alpha) & \cos(\alpha) & \dfrac{[\beta\sinh(\beta)+\alpha\sin(\alpha)]}{(\alpha^2+\beta^2)} & \dfrac{[\beta\cosh(\beta)-\alpha\cos(\alpha)]}{(\alpha^3+\beta^3)} \end{bmatrix} \tag{33}$$

and

$$[\mathrm{P}_n]_t = \begin{bmatrix} 1 & 0 \\ \cos(\tau) & \sin(\tau)/\tau \end{bmatrix}.$$

Then, the $W(\xi)$ and $\Psi(\xi)$ nodal approximations can be rewritten as:

$$\begin{aligned} W(\xi) &=< P(\xi) >_f [P_n]_f^{-1} \{W_n\} =< N(\xi) >_f \{W_n\} \\ \Psi(\xi) &=< P(\xi) >_t [P_n]_t^{-1} \{\Psi_n\} =< N(\xi) >_t \{\Psi_n\} \end{aligned} \tag{34}$$

which represent a nodal approximation of the variables. Similar expressions are also written for the test functions. Expressions (34) can then be rearranged as:

$$\begin{Bmatrix} W(\xi) \\ \Psi(\xi) \end{Bmatrix} = [N]\{w_n\};$$

where, $\{w_n\} =< W_1 \; W'_1 \; \Psi_1 \;\; W_2 \; W'_2 \; \Psi_2 >^T$, and

$$[N] = \begin{Bmatrix} < N(\omega)_f > \\ < N(\omega)_t > \end{Bmatrix} = \begin{bmatrix} N_1(\omega)_f & N_2(\omega)_f & 0 & N_3(\omega)_f & N_4(\omega)_f & 0 \\ 0 & 0 & N_1(\omega)_t & 0 & 0 & N_2(\omega)_t \end{bmatrix}.$$

This equation represents the dynamic shape functions in matrix form (see Appendix B and Figures 3a-d, respectively, for analytical expression of axial, torsional and bending DTSFs and graphical representations of bending DTSFs). Finally,

$$W^k =< \delta w_n > \underbrace{([K_{DS}]^k_{Uncoupl} + [K_{DS}]^k_{Coupl})}_{[K_{DS}]^k} \{w_n\}; \tag{35}$$

where

$$[K_{DS}]^k_{Uncoupl} = \left[c_f \{N_f\}_{\xi=0};\; c_f \{-N_f\}_{\xi=0};\; c_t \{-N_t\}_{\xi=0};\quad c_f \{-N_f\}_{\xi=1};\; c_f \{N_f\}_{\xi=1};\; c_t \{N_t\}_{\xi=1} \right],$$

$$[K_{DS}]^{k}_{coupling} = \begin{bmatrix} 0 & 0 & (Kc)_{11} & 0 & 0 & (Kc)_{21} \\ & 0 & (Kc)_{12} & 0 & 0 & (Kc)_{22} \\ & & 0 & (Kc)_{13} & (Kc)_{14} & 0 \\ & & & 0 & & (Kc)_{23} \\ & Sym. & & & 0 & (Kc)_{24} \\ & & & & & 0 \end{bmatrix}, \tag{36}$$

and

$$(\mathrm{Kc})_{ij} = \int_0^1 C_p N_{it}.N_{jf} + C_{x_\alpha} N_{it}.N_{jf}.d\xi; \quad \text{for } \begin{cases} i = 1,2; \\ j = 1,2,3,4. \end{cases}$$

$$c_f = \frac{H_f}{l_k^3};\ \ c_t = \frac{H_t}{l_k};\ C_p = m x_\alpha l_k \omega^2;\ \ C_{x_\alpha} = \frac{-P x_\alpha}{l_k}.$$

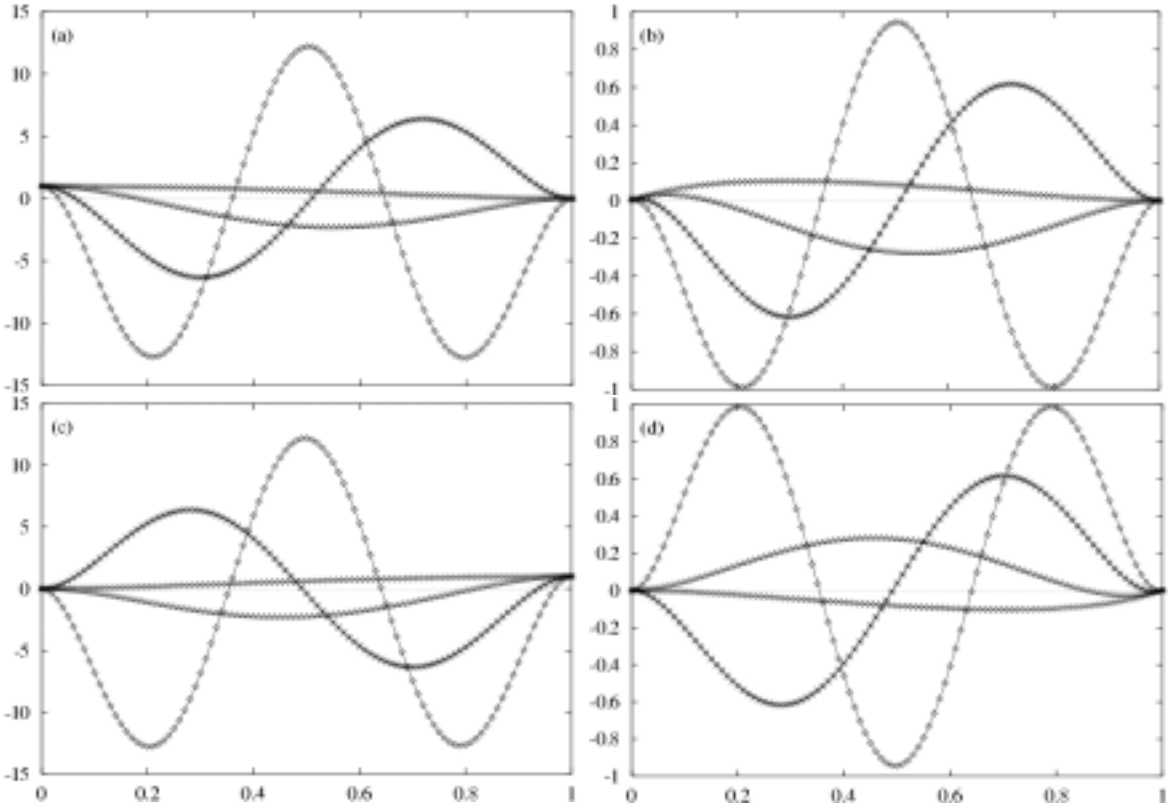

Figure 3 The change of dynamic shape functions N_i, *i =1, 2, 3, 4* vs frequency changes. The first four natural frequencies ω_j, *j* =1,2,3,4 of a uniform beam of *E=1* GPa, *A=1* m^2, *L= 1* m, ρ *= 1* kg/m^3, *I=1* m^4 and a distributed axial force equivalent to a rotating speed of Ω=12 **rad/s is considered.**

3.2.3 Coupled Bending-Torsion Vibration of Beams: DFE Formulation Incorporating Variable Parameters

In a large number of beam vibration problems, the pertinent governing differential equations incorporate variable coefficients, i.e., changes in mechanical and/or geometrical parameters. In those cases, it is impossible or cumbersome to find the 'exact' closed form solution of these equations. For example, let us consider a nonuniform coupled bending-torsion beam in presence of a distributed axial force. An expedient way of dealing with such structure with variable parameters would be to develop an approximate formulation by breaking the structure down into several members, joined end to end, such that the element equations can all presumably have constant coefficients. Then, the constituent members are considered to be straight, uniform, axially pre-stressed elements governed by Bernoulli-Euler bending and St. Venant torsion beam theories (see eqns (2)-(4)). Within each element, the axial force can be taken as constant and equal to the mean value of the true sectional force in that element. Consequently, it will be possible to derive the exact DSM for each member or element based on the approach discussed in section 3.3.1 and Appendix A. Then, the 'approximate' overall stiffness matrix is found by assembling the member DSMs.

Alternatively, the DFE methodology (see sect6ion 3.2.2) can be extended to incorporate the variable parameters into the formulation. For example, let us consider the coupled vibrations of a nonuniform beam with variable bending and torsional rigidities, $H_f(x) = EI(x)$, $H_t(x) = GJ(x)$, and polar moment of inertia, $I_\alpha(x)$, mass per unit length, $m(x) = \rho A(x)$, and a distributed axial load, $P(x)$. Then, one can write

$$H_f(x) = \overline{H_f} + H_f(x)_{delta};\ \ H_t(x) = \overline{H_t} + H_t(x)_{delta};\ \ I_\alpha(x) = \overline{I_\alpha} + I_\alpha(x)_{delta};$$
$$(PI_\alpha / m)(x) = \overline{PI_\alpha / m} + (PI_\alpha / m)(x)_{delta};\ m(x) = \overline{m} + m(x)_{delta};\ \ T(x) = \overline{P} + P(x)_{delta}.$$

where the terms $\overline{H_f}$, $\overline{H_t}$, $\overline{I_\alpha}$, $\overline{m}(x)$ and $\overline{P}$, respectively, are the average 'constant' per element values for variable $H_f(x)$, $H_t(x)$, $I_\alpha(x)$, $m(x)$ and $T(x)$ (see figure 4). New expressions for equations (25) and (26) can then be written as

$$W^e{}_{f\ VARIABLE} = W^e{}_f + \Delta_f, \text{ and } \ W^e{}_{t\ VARIABLE} = W^e{}_t + \Delta_t; \tag{37}$$

where $W^e{}_{f\ VARIABLE}$ and $W^e{}_{t\ VARIABLE}$ stand for element's virtual work incorporating variable parameters for bending and torsion, respectively. $W^e{}_f$ and $W^e{}_t$ are obtained from expressions (27) and (28), respectively, and

$$\Delta_f = -\frac{1}{l_k{}^3}\int_0^1 H_f(x)_{delta}\,\delta w''w''d\xi - \frac{1}{l_k}\int_0^1 P(x)_{delta}\,\delta w'w'd\xi + l_k\omega^2\int_0^1 m(x)_{delta}\,\delta w w d\xi\ ;$$

$$\Delta_t = -\frac{1}{l_k}\int_0^1 \left(H_t(x)_{delta} + (PI_\alpha/m)(x)_{delta}\right)\delta\psi'\psi'd\xi + l_k\omega^2\int_0^1 I_\alpha(x)_{delta}\,\delta\psi\psi d\xi\ .$$

That then leads to a new expression for the element virtual work (see expression 35) as follows:

$$W^k = <\delta w_n> \underbrace{\left([K_{DS}]^k_{Uncoupl} + [K_{DS}]^k_{Coupl} + [K_{DS}]^k_{DEV}\right)}_{[K_{DS}]^k}\{w_n\}; \tag{38}$$

where $[K_{DS}]^k_{Uncoupl}$, and $[K_{DS}]^k_{Coupl}$ are the same as expressions (36) and

$$[K_{DS}]^k_{DEV} = \begin{bmatrix} (\Delta_f)_{11} & (\Delta_f)_{12} & 0 & (\Delta_f)_{13} & (\Delta_f)_{14} & 0 \\ & (\Delta_f)_{22} & 0 & (\Delta_f)_{23} & (\Delta_f)_{24} & 0 \\ & & (\Delta_t)_{11} & 0 & 0 & (\Delta_t)_{12} \\ & & & (\Delta_f)_{33} & (\Delta_f)_{34} & 0 \\ & \textit{Sym.} & & & (\Delta_f)_{44} & 0 \\ & & & & & (\Delta_t)_{22} \end{bmatrix}, \tag{39}$$

$$\begin{aligned} (\Delta_f)_{ij} &= -\frac{1}{l_k{}^3}\int_0^1 H_f(x)_{delta}\,N_{if}{}''N_{jf}{}''d\xi - \frac{1}{l_k}\int_0^1 P(x)_{delta}\,N_{if}{}'N_{jf}{}'d\xi + l_k\omega^2\int_0^1 m(x)_{delta}\,N_{if}N_{jf}d\xi\ ; \\ (\Delta_t)_{kl} &= -\frac{1}{l_k}\int_0^1 \left(H_t(x)_{delta} + (PI_\alpha/m)(x)_{delta}\right)N_{kt}{}'N_{lt}{}'d\xi + l_k\omega^2\int_0^1 I_\alpha(x)_{delta}\,N_{kt}N_{lt}d\xi\ , \end{aligned} \tag{40}$$

for *i, j=1,2,3,4* and *k, l=1,2*.

It can be verified that if the limit of ω (and then η,α,β,τ) $\to 0$, the basis functions $<P>_f \ \to\ <1\ x\ x^2\ x^3>$ and $<P>_a$ (and $<P>_t$) $\to\ <1\ x>$. Consequently the limit of bending shape functions, $<N(x,\omega)>_f$, and also those of the axial (and torsional) interpolation functions, $<N(x,\omega)>_a$ (and $<N(x,\omega)>_t$), respectively, will change to the Hermite cubic shape functions and $<1-x/l\ \ x/l>$. These degenerated basis and shape functions are the same as those frequently used in conventional FEM formulations. As it can be observed, the static stiffness matrix $[k]$ can be obtained from eqns (11, 36) and (39-40), respectively, for beam axial and coupled bending-torsion displacements. Accordingly, the corresponding static mass (interia) matrices, $[m]$, can also be obtained by linearizing the dynamic formulation with respect to ω^2, as presented in [10,11,13].

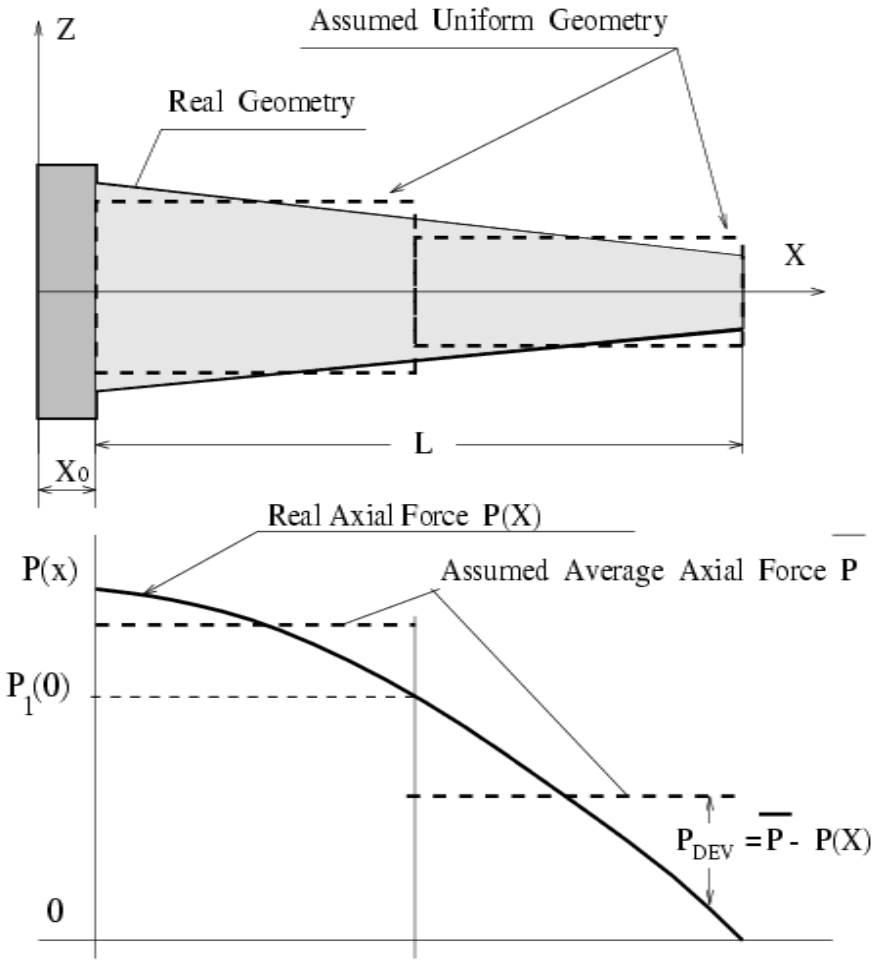

Figure 4 The variable axial force distribution and geometry along a non-uniform beam in *x-y* plane; only two elements are used.

3.3 Global Discretized Form for W

Similar to the classical FEM, each element integral form W^k obtained from the exact DSM or the DFE approach leads to

$$W^k = < \delta u_n > [k(\omega)]\{u_n\}$$

where $[k(\omega)]$ is the frequency dependent element dynamic stiffness matrix for element *k*. Then, the discretized global form of W is equal to the sum of the element virtual works, W^e, for the number of total elements. The standard assembly process is then used:

$$W = \sum_{elements} W^k = < \delta U_n > [K(\omega)]\{U_n\} = 0 \qquad (41)$$

The solution of the problem consists in finding the eigenvalues ω and vectors U_n that make W vanish for any arbitrary $<\delta U_n>$ while satisfying the *boundary conditions* defined on S_u (i.e., $\delta U_i = 0$ and all derivatives of δU_i, $\delta U_i^{(n)} = 0$, where $U_i = \overline{U_i}$, i.e., on the boundaries where all the degrees of freedom U_i have specified values of $\overline{U_i}$). The appropriate boundary conditions can then be introduced in the expression (41) by well-known methods (e.g., direct method, penalty method, etc.).

4 Eigenvalue Calculation and Application of the theory

The DFE developed here, covers the Axial-Bending-Torsion vibrations of nonuniform beams with cross-sections having a single axis of symmetry, and in presence of a distributed axial load. Elementary matrices, $[k_{DS}(\omega)]^k$, derived in the previous sections, will have to be assembled in the usual way to form the overall dynamic stiffness matrix $[k_{DS}(\omega)]$ of the whole structure. The eigenvalue problem resulting from this method, as already mentioned, is then a nonlinear function of frequency, ω, and can be solved to find the structure's natural frequencies and modes of vibration.

4.1 Bisection Method Based on the Sturm Sequence Property of the DSM

Powerful algorithms exist for determining natural frequencies in the case of linear eigenvalue problems, resulting from the discrete or lumped mass models. The use of the Sturm sequence property of the system's eigenproblem, enables one to determine with ease how many natural frequencies lie below any chosen frequency, thereby making it possible to converge on any particular natural frequency and to any required accuracy. Williams and Wittrick [5] presented a comparable method for the type of nonlinear eigenvalue problems mentioned above, where we shall consider undamped, linearly elastic models, and in which the strain energy is a quadratic function of the displacements. The natural frequencies of an infinite system are therefore calculated by varying ω in small steps, calculating the determinant of K_{DS} at each step, and by seeking the values that make the determinant zero. Based on this method, one could also determine the repeated frequencies without any problem. Consequently, the corresponding mode shapes can also be evaluated using the perturbed frequency method and presented in references [5,10].

5 Numerical Tests

Numerical checks are performed to confirm the predictability and accuracy of the theory. The coupled bending-torsional natural frequencies for a variety of open and closed section unloaded beams were studied by substituting $P=0$ in the data and very good agreement was found with published results [6,14,15]. Furthermore, it was also verified that assuming uniform geometry, constant parameters, absence of axial force, $P=0$, and $x_\alpha=0$, the exact natural frequencies of free bending and torsional vibrations of beams can be obtained [16].

In what follows, three illustrative beam configurations, incorporating different coupling effects and variable parameters are presented. First, an example of bending-torsion coupled beam with monosymmetric semi-circular cross-section, given by Friberg (1985) [9] is investigated where the performance of the DFE method in the vibration analysis of systems with geometric couplings is demonstrated. Then, the free vibration of a linearly tapered beam is studied where the variable geometrical parameters are included in the analysis. The third example is a piecewise uniform rotating aluminum blade. In this last test, the performance of the DFE method in the natural frequency calculation of beam structures with distributed (i.e., variable) axial force is shown.

5.1 Monosymmetric Semi-Circular Cross-Section Beam

Numerical results were obtained using an illustrative example of a bending-torsion coupled beam with monosymmetric semi-circular cross-section [9] (see Figure 5 for details). The following cross-sectional properties were used in the calculation:

(i) Average radius, r = 24.5 mm,

(ii) Thickness, t = 4.0 mm,

(iii) The distance between the shear centre and centroid, x_α=15.5 mm,

(iv) Mass per unit length, m = 0.835 kg/m,

(v) Polar mass moment of inertia per unit length, I_α = 501 E^{-6} kg.m,

(vi) Cross-section area, A = 308E^{-6} m^2,

(vii) Second moment of inertia about X-axis, I_{XX} = 92.6 E^{-9} m^4,

(viii) E = 68.9 GPa,

(ix) G = 26.5 GPa, and

(x) The length of the beam, L, was assumed to be 0.82 m.

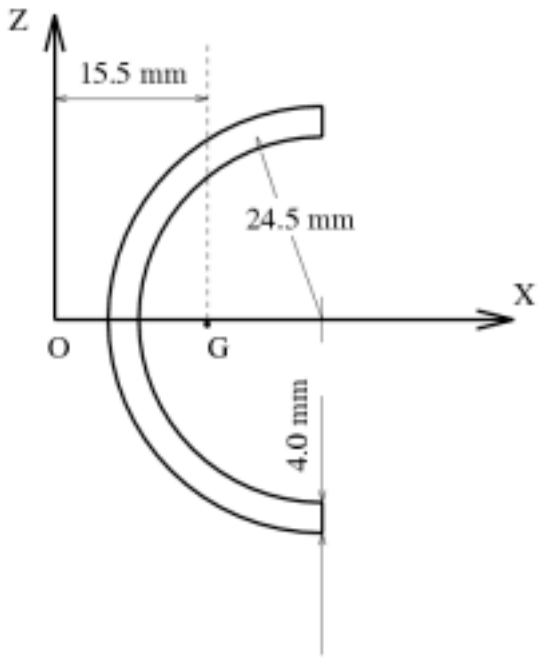

Figure 5 Cross-sectional details of the analyzed bending-torsional coupled beam

First, the Clamped-Free natural frequencies of this example were studied, when the axial force, *P*, is simply assumed to be zero. The natural frequencies obtained from the DFE method, together with the exact results and those found from the classical Finite Elements Method (FEM) are given in Table 1. The exact results are found from the Dynamic Stiffness Matrix (DSM) presented by Banerjee (1989) [6]. The same results can also be obtained from the DSM presented in [7], assuming *P=0*. The classical FEM's results were calculated from the standard Finite Element presented in Reference [17]. A mesh of 200 elements was used where the stiffness and mass matrices were evaluated using a cubic 'Hermite' shape functions for flexural, and linear approximations for torsional displacements. The DFE showed excellent convergences; for the first natural frequency, the error is less than 0.1% even when only four elements are used. The second and third natural frequencies converged to the exact results with approximately 0.1% error and using a mesh of eight elements (The DFE results of Table were found using only five elements).

The effect of a constant axial force on the beam's natural frequencies was then studied. The first three coupled bending-torsional natural frequencies, ω_i, of the beam, with cantilever

end conditions and the compressive axial load *P=-1790* N, were evaluated using the DFE method. The comparison was made between these results and those available in the literature [7,9]. The natural frequencies obtained from DEF, alongside the published exact Dynamic Stiffness Matrix (DSM) [7] and Vlasov's theory results [9], are shown in Table 2. The maximum disagreement between the frequencies obtained from six DEMs and the exact DSM [7] is about 0.2 per cent. The higher difference (6%) between DFE results and those presented in [9] can be attributed to the warping effects (i.e., warping has been neglected in the present theory). However, the errors incurred are expected to be significantly less for closed and solid sections [19]. The warping effect, in this case, plays a relatively minor role. Comparing Tables 1 and 2, one can realize that the beam natural frequencies decrease with a compressive axial load and increase with a tensile force. The beam's first three natural frequencies were found as: f_1 = 64.7, f_2= 132.3 and f_3 = 264.9 (Hz), respectively, when *P=+1790* N. These results are in agreement with an earlier work published by Banerjee and Fisher (1992) [7].

Table 1 Bending-torsional natural frequencies of coupled beam based on present theory[1], exact DSM method[2] and Classical Finite Element[3] (P=0.).

i	DFE [1]	Exact [2]	| Error $_{1-2}$ | **(%)**	Classical FEM [3]	| Error $_{2-3}$ | **(%)**
1	62.5	62.5	0.0	62.6	0.2
2	130.5	130.0	0.4	130.2	0.2
3	261.8	261.0	0.3	261.2	0.1

[1] The results found by using only five Dynamic Finite Elements.
[2] The results obtained using The Exact Dynamic Stiffness Matrix(DSM) method [6,7].
[3] The results obtained using 200 classical Finite Elements Method (FEM) [17].

Table 2 Natural frequencies of axially loaded bending-torsion coupled beam based on present theory[1], exact DSM method[2] and Vlasov theory[3] (P=-1790 N).

I	DFE [1]	Exact [2]	| Error $_{1-2}$ | **(%)**	Vlasov Theory [3]	| Error $_{1-3}$ | **(%)**
1	60.11	60.23	0.20	61.28	1.91
2	128.6	128.4	0.16	136.0	5.44
3	258.4	258.0	0.16	274.9	6.0

[1] The results found by using only six Dynamic Finite Elements.
[2] The results obtained using exact Dynamic Stiffness Matrix (DSM) method [7].
[3] The results obtained using Vlasov's theory [9].

5.2 Linearly Tapered Beam

Here, the free lateral vibration of a linearly tapered beam is presented. The width is assumed to be constant and the height is assumed to have a taper ratio equal to 0.5. The first six natural frequencies, for this case, calculated from different approaches together with the 'exact' results [1] are presented in Table 3. The convergence tests, for the first four natural frequencies, using classical uniform Hermite beam elements (FEM) and DFE are presented in Figure 6. As it can be seen, the DFE method leads to much better convergence rates when compared to the FEM. The DSM method's results are not shown in this figure but, for all of the presented frequencies, DSM method and FEM results produced virtually similar errors; i.e., from Table 3, one observes that when a mesh of 16 classical Hermite beam elements is used, the error is about 0.2%. Similar results are found for the DSM approach (see Figure 6).

Table 3 Non-dimensional natural frequencies of lateral vibration for a tapered beam

μ_I	Exact [a]	FEM [b]	DFE [c]	DSM [d]
μ_1	3.82379	3.82374	3.82278	3.81742
μ_2	18.31726	18.31703	18.31195	18.28127
μ_3	47.26483	47.26419	47.25140	47.16792
μ_4	N.A.	90.44926	90.42473	90.26289
μ_5	N.A.	147.99967	147.96073	147.69569
μ_6	N.A.	219.92054	219.86614	219.47439

[a] The exact results obtained from the variable order FEM method presented in Ref. [1].
[b] The results of the FEM when the wing is broken into 200 static beam elements.
[c] The natural frequencies calculated by DFE, when 16 elements are used.
[d] The natural frequencies calculated by DSM, when 16 elements are used.

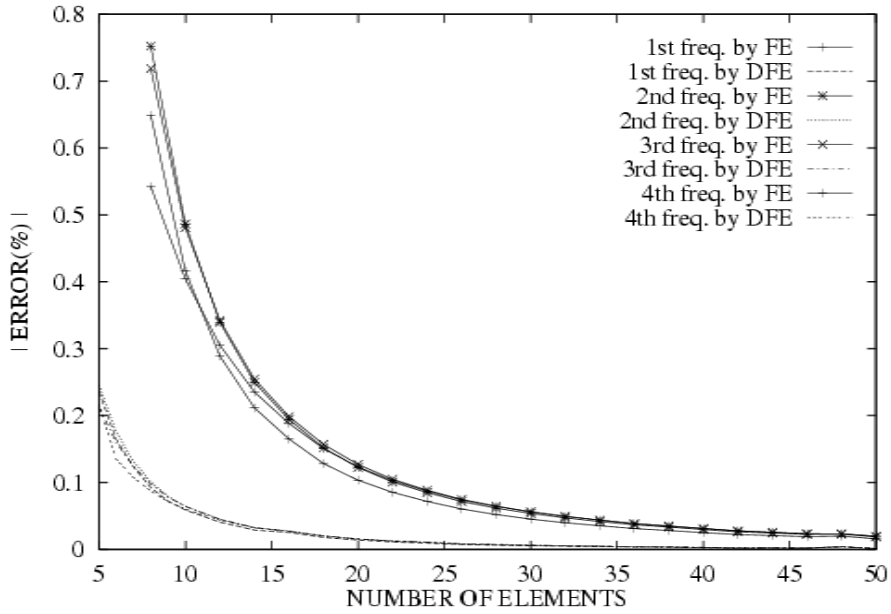

Figure 6 FEM and DFE convergence results for the first four frequencies of lateral vibration for a cantilever linearly tapered beam (taper ratio=0.5).

5.3 Pure Flap-Bending of Piecewise Uniform Rotating Blade

In order to evaluate the merits of the proposed method for the case of a beam-like structure with variable geometrical parameters and distributed axial force, the following example of a rotating aluminum blade with discontinuity in the geometry, was studied.

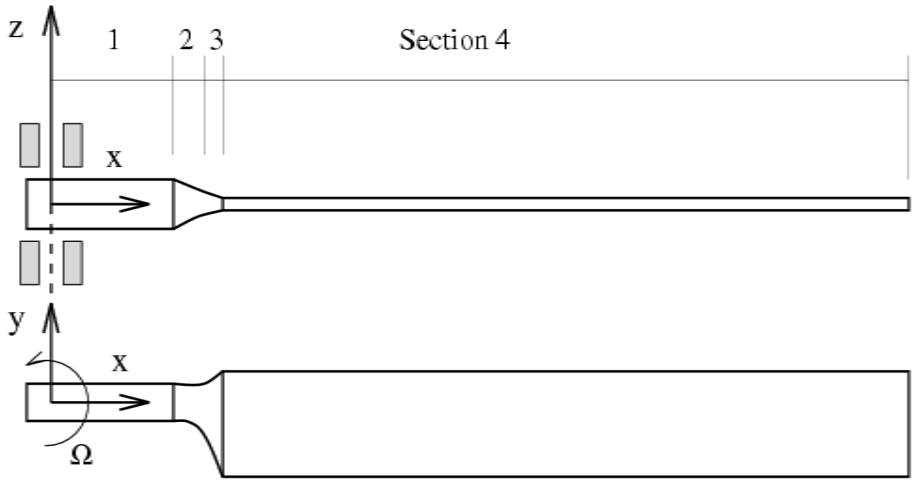

Figure 7 Non-uniform cross-section clamped-free aluminum blade.

Table 4 Model data of an aluminum rotor blade.

Section Number	Length [m]	Area [cm^2]	Mass per unit length, *m*, (Kg/m)	Bending stiffness $N.m^2$
1	0.60	42	11.7054	92106
2	0.12	50	13.9350	76170
3	0.08	51	14.2137	35819
4	4.00	50	13.9350	19006

The blade is assumed to be untwisted and with clamped-free boundary conditions (see Figure 7). The blade model data presented in reference [19] were used and are reproduced in Table 4. The properties of the blade are piecewise constant along the axial co-ordinate. The natural frequencies of lateral flap-bending (out-of-plane of rotation) modes of the blade (Figure 7) are to be evaluated. In reference [19], an "Integral Formulation (I.F.)" based on the use of Green functions (i.e., structural influence functions) was proposed and, using this approach, an analysis of this blade was performed. Here, the first five natural frequencies of this blade are calculated by using different FEM, exact DSM and DFE methods. The results for Ω=0 and Ω=45 rad/sec are presented in Tables 5 and 6, respectively. From Table 5, it can be realized that the FEM results follow the standard pattern of becoming progressively less accurate for higher modes. It was found that, except for the first natural frequency, a mesh of minimum 20 to 30 standard beam elements are required in order to obtain similar results found using only seven DFEs (i.e., higher rates of convergence for the DFE method). The similar tests were carried out for different rotating speeds and the natural frequencies evaluated from DFE approach (using only seven elements), together with corresponding results obtained from the "Integral Formulation (I.F.)" as well as those found from a finite element analysis (reported from Reference [18] of Reference [19]) are presented in Figure 8 and very good agreement was found between these results.

Table 5 Flap-bending natural frequencies of the non-rotating aluminum blade (Ω=0)

ω_I	Reference values [a]	FEM [b]	DSM and DFE [c]
ω_1	1.15533	1.15533	1.15533
ω_2	6.93396	6.93399	6.93397
ω_3	18.5889	18.5894	18.5888
ω_4	34.9951	34.9983	34.9951
ω_5	56.5652	56.5779	56.5653

[a] The natural frequencies calculated by classical FEM, when 194 `Hermite' beam elements are used.
[b] The results of the FEM, using a total of 23 `Hermite' beam elements.
[c] The results of the DFE approach, which in this case is identical to `exact' DSM method, when the blade is discretized by only four elements.

Table 6 Flap-bending natural frequencies of the rotor blade for Ω=45 rad/sec

ω_I	Reference values [a]	FEM [b]	DSM [c]	DFE [d]
ω_1	7.7773	7.77593	7.76655	7.7872
ω_2	19.7035	20.0614	20.009	19.7704
ω_3	35.1293	35.8886	35.8093	35.2116
ω_4	54.9298	56.1962	55.9653	55.0034
ω_5	79.2285	83.1428	81.3068	79.2817

[a] The natural frequencies calculated by classical FEM, when 194 `Hermite' beam elements are used.
[b] The results of the FEM, using a total of seven `Hermite' beam elements.
[c] The results of the DSM, when seven elements are used.
[d] The results of the DFE approach, when the blade is discretized by seven elements.

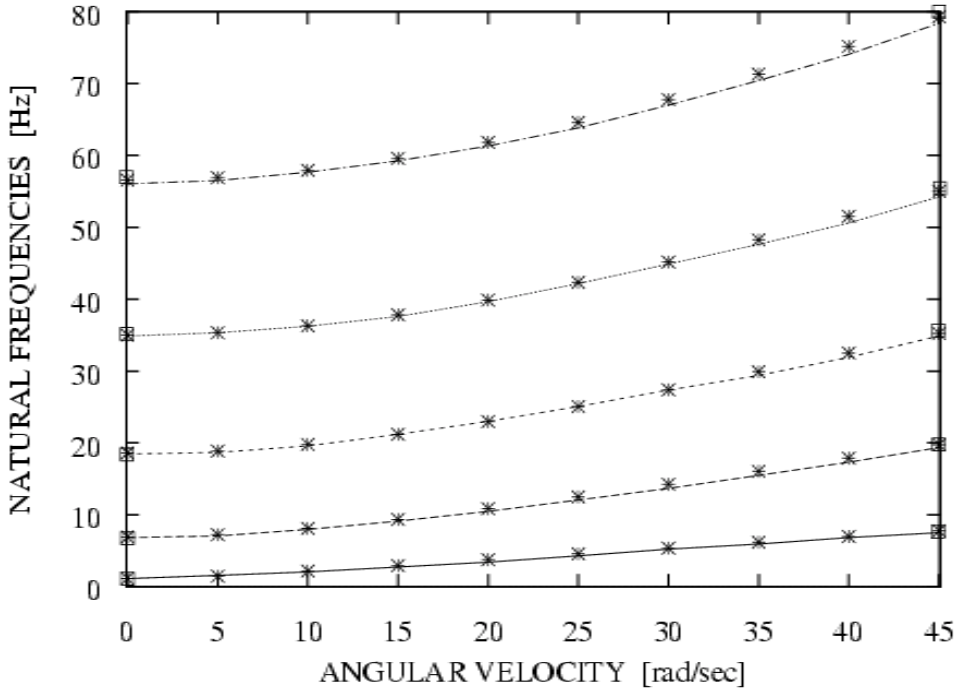

Figure 8 Natural frequencies for flap-bending modes of the aluminum blade. * , DFE results, using seven elements; ----- , Integral Formulation (IF) results presented by Surace et *al.* (1997); , ANSYS results.

6 Discussion and concluding remarks

Exact member (element) equations exist for important structures, including plane frames, space frames, grids, and many plate and shell problems. The frequency dependent Dynamic Stiffness Matrix (DSM) formulation leads to the exact natural frequencies and modes of vibration of structures. In spite of its very accurate results, the most important weakness of the DSM formulation is that it is not a general formulation. The Finite Element Method (FEM), on the other hand, provides a general formulation tool where element matrices are usually evaluated from assumed fixed shape functions. The exact frequency calculation for pure axial, torsional and lateral vibrations of simple beams can be formulated based on the FEM approach when the appropriate Dynamic (frequency dependent) Trigonometric Shape Functions (DTSFs) are used. It was shown that the use of these shape function could bridge the gap between the conventional FEM and the exact DSM approaches. In other words, the FEM formulation can

be directly used to derive the DSM formulation for certain problems [9,10]. On the other hand, the DFE formulation, together with appropriate DTSFs, can be exploited for the vibration modeling and analysis of complex cases where the closed form solution of the governing equations, are not available. The resulting DFE formulation, in this case, is not exact but, since the method shares the generality of FEM method, it can be advantageously exploited to incorporate further mechanical and geometrical complexities into the formulation. This distinguishes DFE method from DSM. The DFE approach, when compared to the counterpart conventional FEM, results in higher convergence rates of results.

Acknowledgment

The author wishes to acknowledge the support provided by Ryerson University.

References

[1] Hodges, D. H. and Rutkowski, M. J., 'Free-Vibration Analysis of Rotating Beams by A Variable-order FEM'. *AIAA Journal*, **19(11):** 1459-1466, 1981.

[2] Bielawa, R. L., *'Rotary Wing Structural and Aeroelasticity'*. AIAA Education Series, 1992.

[3] Gupta, K. K. and Lawson, C. L., 'Development of Block Lanczos Algorithm for Free Vibration Abalysis of Spinning Structures'. *International Journal for Numerical Method in Engineering*, **26**: 1029-1037, 1988.

[4] Cleghorn, W. L. and Tabarrok, B., 'Finite Element Formulation of A Tapered Timoshenko Beam for Lateral Vibration Analysis'. *Journal of sound and vibration*, **152(3)**: 461-470, 1992.

[5] Williams, F. W. and Wittrick, W. H., 'Automatic Computational Procedure for Calculating Natural Frequencies of Skeletal Structures'. *International Journal of Mechanical Science*, **12**: 781-791, 1970.

[6] Banerjee, J. R., 'Coupled Bending-Torsional Dynamic Stiffness Matrix for Beam Elements'. *International Journal for Numerical Methods in Engineering*, **28**: 1283-1298, 1989.

[7] Banerjee, J. R., Fisher, S. A., 'Coupled Bending-Torsional Dynamic Stiffness Matrix for Axially Loaded Beam Elements'. *International Journal for Numerical Methods in Engineering*, **33**: 739-751, 1992.

[8] Vlasov, V. Z., *'Thin-Walled Elastic Beams'*, 2nd edition, Moscow 1959.

[9] Friberg, P. O. 'Beam Element Matrices Derived From Vlasov's Theory of Open Thin-Walled Elastic Beams'. *International Journal for Numerical Methods in Engineering*, **21**: 1205-1228, 1985.

[10] Hashemi, S. M., '*Free Vibrational Analysis of Rotating Beam-like Structures: A Dynamic*

Finite Element Approach'. Ph.D. Dissertation, Department of Mechanical Engineering, Laval University, Québec, Canada, 1998.

[11] Hoorpah, W., Henchi, K. and Dhatt, G., 'Calcul exact des fréquences de vibration des structures *à* poutres par les matrices de rigidité dynamiques application aux ponts mixtes bipoutres'. *Construction Métalique*, **4**: 19-41, 1994.

[12] Przemieniecki, J. S., '*Theory of matrix structural analysis'*, McGraw-Hills Inc.: New York, 1968.

[13] Leung A.Y.T., '*Dynamic Stiffness and Substructures*', Springer-Verlag, London, 1993.

[14] Goland, M. 'Flutter of A Uniform Cantilever Wing'. *Journal of Applied Mechanics*, **12**: A197-A208, 1945.

[15] Eslimi-Isfahani S. H. R., Banerjee J. R. and Sobey A. J. 'Response of A Bending-Torsion Coupled Beam To Deterministic and Random Loads'. *Journal of Sound and Vibration*, **195(2)**: 267-283, 1996.

[16] Wittrick W. H. and Williams F. W. 'A General Algorithm for Computing Natural Frequencies of Elastic Structures'. *Quarterly Journal of Mechanics and Applied Mathematics*, **24**: 263-284, 1971.

[17] Hallauer W. L. and Liu R. Y. L. '*Beam Bending-Torsion Dynamic Stiffness Method for Calculation of Exact Vibration Modes'*. *Journal of Sound and Vibration*, **85**: 105-113, 1982.

[18] K. B. Subrahmanyam, S. V. Kulkarni and J. S. Rao, 'Application of The Reissner Method to Derive The Coupled Bending-Torsion Equations of Dynamic Motion of Rotating Pretwisted Cantilever Blading with Allowance for Shear Deflection, Rotary Inertia, Warping and Thermal Effects'. *Journal of Sound and Vibration*, **84(2)**: 223-240, 1982.

[19] Surace, G., Anghel, V. and Mares, C., 'Coupled Bending-Bending-Torsion Vibration Analysis of Rotating Pretwisted Blades: An Integral Formulation and Numerical Examples'. *Journal of Sound and Vibration*, **206(4)**: 473-486, 1997.

APPENDIX A: EXACT DSM FORMULATION FOR COUPLED BENDING-TORSION VIBRATION OF AXIALLY LOADED EULER-BERNOULLI–ST.VENANT BEAMS

Consider the prestressed beam coupled bending-torsion vibrations governed by equations (3,4) [8]. If the beam is idealized as the assembly of elements with homogeneous material and uniform geometry, then these equations can be written as

$$H_f w''' - P(w'' - x_\alpha \psi'') - m\omega^2 (w - x_\alpha \psi) = 0 \tag{A1}$$

$$H_t \psi'' + P[(I_\alpha / m) - x_\alpha w''] + I_\alpha \omega^2 \psi - m x_\alpha \omega^2 w = 0 \tag{A2}$$

where $w(x)$ and $\psi(x)$ are the amplitude of the sinusoidally varying torsional and transverse displacements, respectively. Appropriate boundary conditions are to be applied at $x = 0$ and $x = L$. Equations (A1–2) can be combined into one equation by eliminating either w or ψ to give the sixth order differential equation as

$$\left(D^6 + aD^4 - bD^2 - c\right)W = 0 \tag{A3}$$

where

$$W = w \text{ or } \psi; \quad D = d/d\xi; \quad \xi = x/l$$

and

$$a = \bar{a}\bar{b} + \bar{p}(\bar{b} - \overline{apc})\}/\ (\bar{b} - \overline{ap})b = \bar{b}(\bar{b} - 2\overline{apc})\ /\ (\bar{b} - \overline{ap})c = \bar{a}\bar{b}^2\bar{c}\ /\ (\bar{b} - \overline{ap}) \tag{A4}$$

with

$$\bar{p} = -Pl^2/EI\bar{a} = I_\alpha \omega^2 l^2\ /\ GJ\bar{b} = m\omega^2 l^4\ /\ EI\bar{c} = 1 - m x_\alpha^2\ /\ I_\alpha \tag{A5}$$

The solution of the differential equation (3) obtained as [6,10]

$$W(\xi) = C_1 \cosh\alpha\xi + C_2 \sinh\alpha\xi + C_3 \cos\beta\xi + C_4 \sin\beta\xi + C_5 \cos\gamma\xi + C_6 \sin\gamma\xi = < P(\xi) > \{C\} \tag{A6}$$

where $C_1 - C_6$ are constants and

$$\left.\begin{aligned} \alpha &= [2(q/3)^{1/2} \cos(\phi/3) - a/3]^{1/2}; \\ \beta &= [2(q/3)^{1/2} \cos(\pi - \phi)/3 + a/3]^{1/2}; \\ \gamma &= [2(q/3)^{1/2} \cos(\pi + \phi)/3 + a/3]^{1/2}; \end{aligned}\right\} \tag{A7}$$

with

$$q = b + a^2/3 \quad \phi = \cos^{-1}[(27c - 9ab - 2a^3)/2(a^2 + 3b)^{3/2}] \tag{A8}$$

$W(\xi)$ can then be used to write the expressions for both w and ψ by choosing appropriate coefficients $C_i = A_i$, and $C_i = B_i$, for $i = 1,..,6$, where A_i and B_i are the two different sets of constants and they are related to each other [6]. The expressions for counterclockwise rotation θ, the bending moment $M(\xi)$, the shear force $S(\xi)$ and the torque $T(\xi)$ are written as

$$\left.\begin{aligned} &\theta(\xi) = w'(\xi)/l; \qquad M(\xi) = -(EI/l^2)w''(\xi); \\ &S(\xi) = (EI/l^3)w'''(\xi) - (P/l)\{w'(\xi) - x_\alpha\psi(\xi)\} \\ &T(\xi) = (GJ + PI_\alpha/m)\psi'(\xi)/l - (Px_\alpha/l)w'(\xi) \end{aligned}\right\} \tag{A9}$$

The end conditions for displacements and forces of the beam element are

at end 1 (i.e., at $\xi = 0$); $w = w_1, \theta = \theta_1$ and $\psi = \psi_1$,
at end 2 (i.e., at $\xi = 1$); $w = w_2, \theta = \theta_2$ and $\psi = \psi_2$,
at end 1 (i.e., at $\xi = 0$); $S = S_1, M = M_1$ and $T = -T_1$,
at end 2 (i.e., at $\xi = 1$); $S = -S_2, M = -M_2$ and $T = T_2$.

Substituting displacement end conditions in eqn (A6) and the first expression in (A9), and force end conditions in the rest of expressions in (A9), respectively, gives

$$U_n = BA \tag{A10}$$

and

$$F = DA \tag{A11}$$

where

$\{U_n\} = [w_1\ \theta_1\ \psi_1\ w_2\ \theta_2\ \psi_2]^T$; $\{A\} = [A_1\ A_2\ A_3\ A_4\ A_5\ A_6]^T$; $\{F\} = [S_1\ M_1 T_1\ S_2\ M_2\ T_2]^T$

Finally, the dynamic stiffness matrix is found as:

$$K = DB^{-1} \tag{A12}$$

More detailed development of the method and also the explicit matrix form of expressions $[B]$ and $[D]$ are presented in [6].

APPENDIX B: Dynamic (Frequency Dependent) Shape Functions

The extensional dynamic shape functions are found to be as

$$N_1(\omega)_a = \cos(\eta\xi) - \cos(\eta)\frac{\sin(\eta\xi)}{D_a}; N_2(\omega)_a = \frac{\sin(\eta\xi)}{D_a};$$

and torsional dynamic shape functions are

$$N_1(\omega)_t = \cos(\tau\xi) - \cos(\tau)\frac{\sin(\tau\xi)}{D_t}; N_2(\omega)_t = \frac{\sin(\tau\xi)}{D_t};$$

The dynamic flexural shape functions are found to be as follows [10]:

$$N_1(\omega) = \frac{(\alpha\beta)}{D_f}[-\cos(\alpha\xi) + \cos(\alpha(1-\xi))\cosh(\beta) + \cos(\alpha)\cosh(\beta(1-\xi)) - \cosh(\beta\xi) - \frac{\beta}{\alpha}\sin(\alpha(1-\xi))\sinh(\beta) + \frac{\alpha}{\beta}\sin(\alpha)\sinh(\beta(1-\xi))];$$

$$N_2(\omega) = \frac{1}{D_f}[\beta(\cosh(\beta(1-\xi))\sin(\alpha) - \cosh(\beta)\sin(\alpha(1-\xi)) - \sin(\alpha\xi)) + \alpha(\cos(\alpha(1-\xi))\sinh(\beta) - \cos(\alpha)\sinh(\beta(1-\xi)) - \sinh(\beta\xi))];$$

$$N_3(\omega) = \frac{(\alpha\beta)}{D_f}[-\cos(\alpha(1-\xi)) + \cos(\alpha\xi)\cosh(\beta) - \cosh(\beta(1-\xi)) + \cos(\alpha)\cosh(\beta\xi) - \frac{\beta}{\alpha}\sin(\alpha\xi)\sinh(\beta) + \frac{\alpha}{\beta}\sin(\alpha)\sinh(\beta\xi)];$$

$$N_4(\omega) = \frac{1}{D_f}[\beta(-\cosh(\beta\xi)\sin(\alpha) + \sin(\alpha(1-\xi)) + \cosh(\beta)\sin(\alpha\xi)) - \alpha(\cos(\alpha\xi)\sinh(\beta) + \sinh(\beta(1-\xi)) + \cos(\alpha)\sinh(\beta\xi))];$$

where

$$D_f = (\alpha\beta)[-2(1-\cos(\alpha)\cosh(\beta)) + (\frac{\alpha^2-\beta^2}{\alpha\beta})\sin(\alpha)\sinh(\beta)]; D_a = \sin(\eta); D_t = \sin(\tau);$$

$$\alpha, \beta = \frac{1}{\sqrt{2A}}|-B \pm |B^2 - 4A*C|^{\frac{1}{2}}|^{\frac{1}{2}};$$

$$\eta = \omega l_k (m/H_a)^{1/2}; \tau = \omega l_k R(m/H_t)^{1/2}; \quad A = \frac{H_f}{l_k^3}; B = -(\frac{P}{l_k}); C = -ml_k(\omega^2).$$